Glycylglycine $\pi\rightarrow\pi^*$ and Charge Transfer Transition Moment Orientations: Near-Resonance Raman Single-Crystal Measurements

Vasil Pajcini,[†] X. G. Chen,[†,§] Richard W. Bormett,[†] Steven J. Geib,[†] Pusheng Li,[†] Sanford A. Asher,*[,†] and Edward G. Lidiak[‡]

Contribution from the Departments of Chemistry and of Geology and Planetary Science, University of Pittsburgh, Pittsburgh, Pennsylvania 15260

Received May 21, 1996[⊗]

Abstract: We have grown a novel crystal of hydrated gycylglycine (Gly-Gly), determined its crystal structure, and measured its Raman tensor at 488, and 244 nm, close to resonance. This crystal has 8 molecules of (Gly-Gly) and 12 molecules of water per unit cell. The Gly-Gly hydrogen-bonds in a β-sheet-like structure where all of the amide planes are parallel. We report here the development of a general method to use preresonance single-crystal Raman measurements to determine the direction of the molecular electronic transition moments. We utilize the UV (244 nm) excited Raman tensor and relationships derived here to accurately determine the transition moment orientation of the amide and carboxylate group $\pi\rightarrow\pi^*$ transitions and the orientation of a charge transfer transition from the carboxylate group to the amide group. The amide $\pi\rightarrow\pi^*$ (NV_1) transition moment is found to be in the peptide plane at an angle of $-46° \pm 3°$ to the amide carbonyl bond. The carboxylate $\pi\rightarrow\pi^*$ (NV_1') transition moment is oriented almost parallel to a line connecting the carboxylate oxygens (4.6° off), as theoretically expected. The charge transfer band from the carboxylate to the amide chromophore is found at an angle of $-83° \pm 3°$ to the amide carbonyl bond, almost along the line of intersection of the amide and carboxylate planes.

Introduction

A fundamental understanding of the structure and dynamics of peptides and proteins, and the development of calculational methodologies to predict protein structure and reactivity, require a detailed understanding of the molecular bond force constants and dynamics. This understanding must be built upon a deeper insight into the structure and dynamics of the molecular fragments which make up the peptide or protein structure. This has motivated the numerous incisive investigations of small molecules like *N*-methylacetamide, propanamide, *N*-acetylglycine, glycylglycine, etc. Both ground and excited state structure and dynamics are important, since the ground state specifies the likely conformation in an unconstrained environment, while the excited states govern the proclivity of the molecular fragment to be strained into particular geometries or to undergo unusual dynamics in challenging environments.

The ground state conformation of molecules can be characterized directly by techniques such as X-ray diffraction and 2-D NMR or indirectly by using spectroscopic methods such as vibrational spectroscopy, electronic spectroscopy, CD, NMR, etc. or by chemical reactivity methodologies. Excited state geometries and dynamics can be determined only through spectroscopic investigations or, with uncertain reliability by emerging theoretical calculational techniques. The relevant information required is the energies of the ground and excited states, the equilibrium geometries, and their potential functions along the relevant molecular dynamical coordinates.

The great difficulty of these types of investigations for protein fragments such as the amide linkage is that the electronic excited states occur in the deep UV, which is a congested spectral region; UV absorption methods give broad bumps which are difficult to interpret. Partial deconvolution of these broad bumps is possible using electronic dichroism measurements that monitor the directions of the electronic transition moments. For example, Clark's recent linear dichroism measurement of propanamide and *N*-acetylglycine[1] and previous measurements of *N*-acetylglycine[2] and myristamide[3] have given important information on the amide group excited states.

At present, the frontier amide and dipeptide excited states are thought to give rise to low-energy *ca*. 220 nm weak $n\rightarrow\pi^*$ transitions of the amide and carboxylate groups, a *ca*. 190 nm strong $\pi\rightarrow\pi^*$ amide transition, and a *ca*. 160 nm strong carboxylate $\pi\rightarrow\pi^*$ transition.[4] We have recently identified in dipeptides a *ca.* 200 nm charge transfer transition from the carboxylate nonbonding orbital to the amide π^* orbital.[5] Other $\pi\rightarrow\pi^*$ transitions and Rydberg transitions have been suggested to occur at higher energies.

In the work here, we utilize single-crystal UV near-resonance Raman spectroscopy to incisively probe the electronic transitions of the dipeptide glycyglycine. Raman spectroscopy examines the ground state vibrational spectrum of a molecule by examining the inelastic scattering of light from a collection of molecules. The photon is shifted by a vibrational frequency due the coupling of the nuclear vibrational motion to the electronic motion. Excitation of the Raman spectra in resonance with a particular electronic transition selectively probes those vibrations coupled to the electrons involved in the electronic transition. This information can be used to detect the atomic

[†] Department of Chemistry.
[‡] Department of Geology and Planetary Science.
[§] Present address: Section on Metabolic Analysis and Mass Spectrometry, NICHD, National Institutes of Health, 10 Center Dr., MSC 1580, Building 10, Room 6C208, Bethesda, MD 20892.
[⊗] Abstract published in *Advance ACS Abstracts,* September 15, 1996.

(1) Clark, L. B.; *J. Am. Chem. Soc.* **1995,** *117*, 7974.
(2) Ward, J. C. *Proc. R. Soc. London* **1955,** *A228*, 205.
(3) Peterson, D. L.; Simpson, W. T. *J. Am. Chem. Soc.* **1957**, *79*, 2375.
(4) (a) Basch, H.; Robin, M. B.; Kuebler, N. A. *J. Chem. Phys.* **1967**, *47*, 1201. (b) Robin, M. B. *Higher Excited States of Polyatomic Molecules*; Nonaromatic Unsaturates; Academic Press: Orlando, FL, 1975; Vol. II, Chapter 5, pp 121−160.
(5) Chen, X. G.; Li, P.; Holtz, J. S. W.; Chi, Z.; Pajcini, V.; Asher, S. A.; Kelly, L. A. *J. Am. Chem. Soc.* **1996**, *118*, 9705 (preceding paper in this issue).

S0002-7863(96)01725-8 CCC: $12.00

localization of an electronic transition if the particular vibrations probed are localized in particular regions of the molecule.

Single-crystal Raman measurements give the orientation of the axes of the diagonal molecular Raman tensor for each vibration observed. Previous biological single-crystal Raman studies,[6−13] including the single-crystal amide studies of Tsuboi *et al.*[8,12] and others,[7] related the Raman tensor in the crystal frame to that in the molecule. These studies, which occurred far from resonance, monitored the normal Raman polarizability. The orientation of the normal Raman polarizability in the molecular frame is controlled by a host of interactions between the vibrational modes and the various electrons which constitute the molecular electron cloud.

We have chosen to selectively probe the *resonance Raman tensor* by exciting sufficiently close to the electronic transition as to be dominated by it, but not so close as to have too much absorption, heating, and decomposition. The resonance Raman tensor can be directly related to the resonant electronic transition moment orientation. Each vibration possesses its own tensor, and the rich information available in resonance allows us to resolve the underlying components of the UV absorption bands and to determine the directions of the transition moments. We believe our study, reported here, is the first to use near-resonance Raman excitation to force the dominance of one resonant transition for the Raman scattering. This allows us to determine the direction of the electronic transition moment from the measured Raman tensor elements.

For glycylglycine, we have determined the directions of the amide and the carboxylate $\pi \rightarrow \pi^*$ transitions and the charge transfer transition from the carboxylate to the amide chromophore. These frontier transitions give rise to the UV absorption of amides, the CD absorption bands, and the UV resonance Raman enhancement. The excited states utilize the same unfilled molecular orbitals as those utilized in protein electron transfer. Our results should represent a challenge to the theoretical community to prove the reliability of electronic structure calculations.

Experimental Section

Crystal Growth and Structure Determination. Glycylglycine (free base, pH range 7.5−8.9) was purchased from Sigma Chemical Co. and was used without further purification. Crystals of glycylglycine (Gly-Gly) grew by slow evaporation of saturated aqueous solutions in covered Petri dishes. We grew a large 13 mm × 10 mm × 3 mm single crystal for this study by using a small Gly-Gly seed crystal.

The monoclinic, space group $C_{2/c}$ crystals had the empirical formula $C_4H_8N_2O_3 \cdot 1.5H_2O$ and contained 8 molecules of Gly-Gly and 12 molecules of H_2O per unit cell. The unit cell dimensions were a = 15.929(3) Å, b = 4.7707(0) Å, and c = 19.414(4) Å, with angles of α = 90°, β = 109.895(14)°, and γ = 90°. The Gly-Gly molecule occupied a site symmetry of C_1, while the factor group symmetry was C_{2h}^6. Figure 1 shows the molecular structure of Gly-Gly and the molecular orientation within the unit cell.

Identical environments occur for each Gly-Gly molecule in the crystal. All of the oxygen atoms are hydrogen-bonded. The amide hydrogen of each Gly-Gly H-bonds to the amide carbonyl oxygen of the neighbor Gly-Gly with an H-bond length of 2.128 Å. The carboxylate O(1) atom is H-bonded to two different H_2O molecules with bond lengths of 1.900 and 1.965 Å, respectively. The carboxylate O(2) atom H-bonds to the NH_3^+ group of an adjacent Gly-Gly with an H-bond length of 2.067 Å and H-bonds to another molecule of H_2O with an H-bond length 1.912 Å.

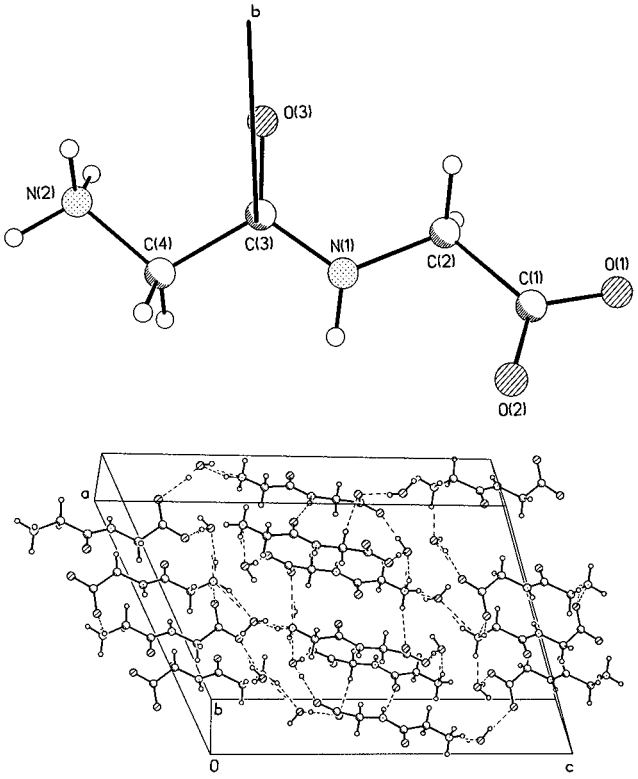

Figure 1. (a) X ray crystal structure of Gly-Gly showing the orientation of the crystallographic *b* axis. (b) Gly-Gly ($8C_4H_8N_2O_3 \cdot 12H_2O$) unit cell.

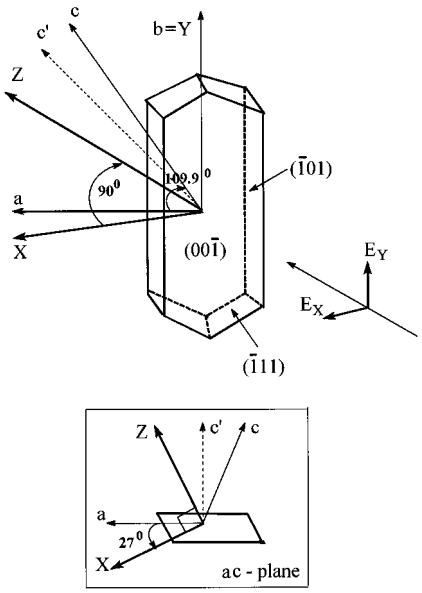

Figure 2. Gly-Gly single crystal showing orientation of optic axes (the $b = Y$ crystallographic axis is perpendicular to the a and c crystallographic axes. c' is an axis perpendicular to the a and b axes. X and Z are the optic axes, and XYZ are the axes of the laboratory Cartesian coordinate system. The polarized excitation and Raman scattered light propagates along the Z optic axis.

We used a Stoe two-circle optical goniometer[14] to index the crystal faces (Figure 2). The big hexagonal face was found to be (00$\bar{1}$). The long edge plane parallel to the *b* axis, which was inclined at 63° to the (00$\bar{1}$) face, was indexed as the ($\bar{1}$01) plane. The smallest face at the

(6) Higgs, P. W. *Proc. R. Soc. London* **1953**, *A220*, 427.
(7) Wilser, W. T.; Fitchen, D. B. *J. Chem. Phys.* **1975**, *62*, 720.
(8) Tsuboi, M.; Ikeda, T.; Ueda, T. *J. Raman Spectrosc.* **1991**, *22*, 619.
(9) Ueda, T.; Ushizawa, K.; Tsuboi, M. *Spectrochim. Acta* **1994**, *50A*, 1661.
(10) Tsuboi, M.; Ueda, T.; Ushizawa, K.; Nagashima, N. *J. Raman Spectrosc.* **1995**, *26*, 745.
(11) Benevides, J. M.; Tsuboi, M.; Wang, A. H.-J.; Thomas, G. J., Jr. *J. Am. Chem. Soc.* **1993**, *115*, 5351.
(12) Tsuboi, M.; Ueda, T.; Ushizawa, K. *J. Mol. Struct.* **1995**, *352*, 509.
(13) Thomas, G. J., Jr.; Benevides, J. M.; Overman, S. A.; Ushizawa, K.; Saitoh, M.; Tsuboi, M. *Biophys. J.* **1995**, *68*, 1073.
(14) Groth, P. H. *Chemiche Krystallographie;* Engelman: Leipzig, 1906; pp 1−626.

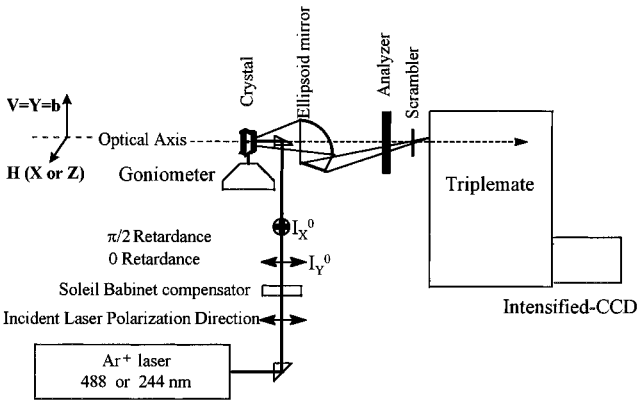

Figure 3. Block diagram of the experimental setup for the polarized Raman crystal measurements.

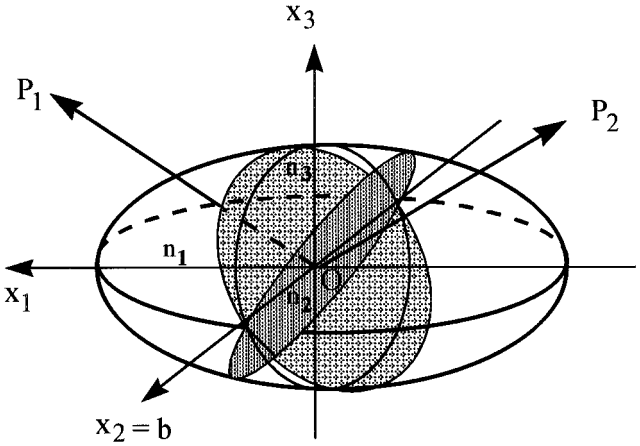

Figure 4. Polarizability ellipsoid of a biaxial crystal showing the two optic axes OP_1 and OP_2, which are perpendicular to the circular sections (adapted from Nye[17]).

corner of the crystal has the index $(\bar{1}11)$. Figure 2 shows the orientation of the three crystallographic axes *a*, *b*, and *c*, where the *b* axis is a two-fold symmetry axis.

Spectroscopic Instrumentation. The visible and UV Raman spectra were obtained by using a 180° backscattering geometry (Figure 3). Excitation at 488 nm was obtained from a Coherent Innova 300 Ar^+ laser. UV excitation at 244 nm was obtained by intracavity doubling the 488 nm line with a BBO crystal.[15] The output laser beams were linearly polarized. We used a quartz Soleil-Babinet compensator (Optics for Research) to produce the desired orthogonal polarizations.

The laser power at the crystal was 50 mW for 488 nm excitation, and we accumulated each spectrum for 20 s. For 244 nm excitation, the laser power at the crystal was 0.5 mW, and the spectra were accumulated for 50 s.

The ellipsoidal mirror used to collect the scattered light utilized a solid angle of less than 0.2 str (0.06π str). A calibrated Polacoat polarization analyzer was placed after the ellipsoidal mirror. The polarization analyzer was oriented to pass either vertically or horizontally polarized light. The combination of the Soleil-Babinet compensator and the polarization analyzer allowed us to measure VV, VH, HV, and HH spectra without moving the Gly-Gly crystal.

A polarization scrambler was placed before the spectrometer entrance slit to randomize the polarization entering the spectrometer. A Spex Triplemate monochromator dispersed the light, which was detected by an intensified CCD detector (Princeton Instrument Co.).

Prior to the experiment, we checked the polarization measurements by determining the depolarization ratios[16] of CCl_4 and CH_3CN. These depolarization ratios were determined by measuring the intensities of the four combinations of the Soleil-Babinet compensator setting and Polacoat analyser setting, I_{HH}, I_{HV}, I_{VH}, and I_{VV}.

The Gly-Gly crystal was mounted in a goniometer, with the $(00\bar{1})$ face perpendicular to the direction of the exciting beam and the *b* crystallographic axis oriented vertically (Figure 3). We defined the *b* axis to be the *Y* axis of the laboratory Cartesian coordinate system. The goniometer allowed us to rotate the crystal around the three perpendicular axes.

Monoclinic crystals are biaxial, and the polarization of light inside the crystal is preserved only for light which propagates along the two optic axes. The crystal birefringence complicates the Raman polarization measurements, since we have to avoid depolarization of both the exciting and scattered light inside the crystal.

A biaxial crystal has three principal refractive indices, n_1, n_2, and n_3, and its indicatrix ellipsoid has three perpendicular semiaxes, Ox_1, Ox_2, and Ox_3, of lengths n_1, n_2, and n_3, respectively[17,18] (Figure 4). The biaxial indicatrix ellipsoid has two circular sections, whose intersection contains the $x_2 \equiv Y \equiv b$ crystallographic axis of our crystal. The optic axes OP_1 and OP_2 lie normal to the planes of these circular sections. The optic plane that contains the optic axes OP_1 and OP_2 is perpendicular to the $b = Y$ principal axis of the indicatrix ellipsoid.

Plane-polarized light that propagates along an optic axis preserves its polarization; the refractive index is n_2 for all orientations of the electrical vector (Figure 4). In contrast, plane-polarized light that propagates along one of the principal axes Ox_1, Ox_2, or Ox_3 conserves the polarization state only if the electric vector lies along another principal axis. Neither the optic axes nor the principal axes generally coincide with the crystallographic axes. In a monoclinic crystal, the crystallographic axis *b* is always a principal axis,[18] but the optic axes do not coincide with the crystallographic axes. We preserved the polarization of the exciting and Raman scattered light by utilizing a geometry where the excitation and scattered light both propagate along an optic axis.

The Gly-Gly crystal optic axes were determined by using a polarizing optical microscope. These axes were perpendicular to the $b = Y$ axis; thus, the optic axes lie in the *ac* plane (horizontal plane in our measurements). One of them, *X*, forms a 27° angle with the *a* crystallographic axis,[19] while the other, *Z*, is perpendicular to *X* (Figure 2). Thus, we used the two optic axes and the *b* crystallographic axis as our laboratory Cartesian system *XYZ*. This was a fortunate case for our study, but even in the general case, when the optic axes are not perpendicular to each other, it is possible to do similar Raman polarization measurements (for more details, see Appendix B).

To avoid birefringence, we oriented the crystal with its *Z* optic axis parallel to the propagation direction of the exciting beam, inside the crystal. We rotated the $(00\bar{1})$ face counterclockwise around the $b = Y$ axis by 39°, to compensate for refraction.

In this geometry, the electric vector of the exciting beam occurred either along the *X* or *Y* direction (Figure 2). By rotating the polarization analyzer, we examined scattered light polarized either in the horizontal or the vertical direction. Thus, we measured the $Z(XX)\bar{Z}$, $Z(XY)\bar{Z}$, $Z(YX)\bar{Z}$, and $Z(YY)\bar{Z}$ Raman spectra.

Next, we rotated again the crystal around the *b* axis in order to bring the $(\bar{1}01)$ face perpendicular to the exciting beam, and the *X* optic axis became parallel to the direction of the exciting beam. By the same procedure, we recorded the $X(ZZ)\bar{X}$, $X(ZY)\bar{X}$, $X(YZ)\bar{X}$, and $X(YY)\bar{X}$ Raman spectra.

We experimentally searched for changes in the optic axes orientation between the visible and UV Raman measurement by adjusting the crystal orientation such that the measured $Z(XY)\bar{Z}$ and $Z(YX)\bar{Z}$ were identical. We found a change of less than our angular resolution (<1°). This is the expected result for our case, in that the orientations of the optic axes are determined by the directions of the maximum projections of the amide $\pi \rightarrow \pi^*$ and the charge transfer transitions of the molecules in the unit cell. These two transitions have almost identical frequencies, and these transitions dominate both the visible and the UV optical properties. The optic axes refractive index dispersions are almost identical, and little rotation of these axes is expected between the visible and UV.

(15) Asher, S. A.; Bormett, R. W.; Chen, X. G.; Lemmon, D. H.; Cho, N.; Peterson, P.; Arrigoni, M.; Spinelli L.; Cannon, J. *Appl. Spectrosc.* **1993,** *47,* 628.

(16) DeVito, V. L.; Cai, M. Z.; Asher, S. A.; Kehres, L. A.; Smith, K. M. *J. Phys. Chem.* **1992**, *96,* 6917.

(17) Nye, J. F. *Physical Properties of Crystals*; Clarendon Press: Oxford, 1957; pp 235−238.

(18) Wahlstrom, E. E. *Optical Crystallography*; John Wiley & Sons: New York, 1960; pp 207−244.

(19) *X* and *Z* are used here to label the optic axes; they should not be confused with the labels for the principal axes of ref 18.

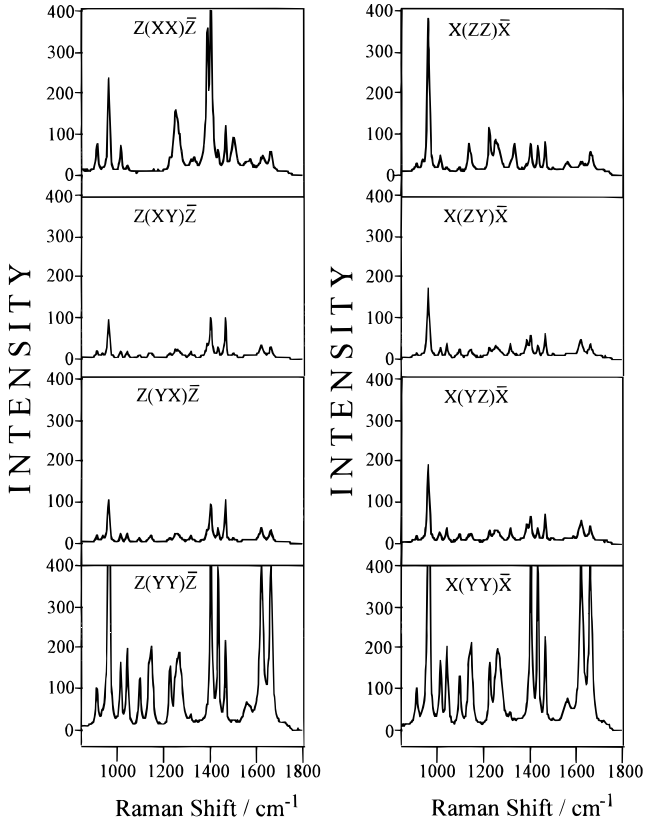

Figure 5. Visible Raman spectra of Gly-Gly crystal (denoted using Porto notation).

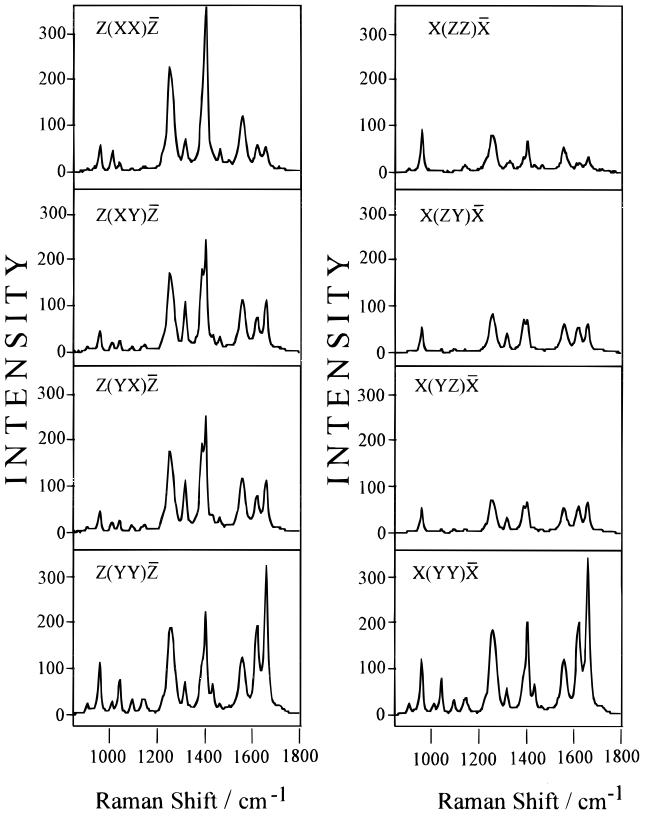

Figure 6. UV Raman spectra of Gly-Gly crystal (denoted using Porto notation).

Results

The visible and UV polarized Raman spectra of the Gly-Gly crystal are shown in Figures 5 and 6, where the spectra are denoted using the Porto notation.[20] The $Z(XY)\bar{Z}$ and $Z(YX)\bar{Z}$ spectra are identical to each other, as are the $X(ZY)\bar{X}$ and $X(YZ)\bar{X}$ spectra. This expected result comes from the fact that the Raman tensor is symmetric and experimentally verifies the accuracy of our polarization Raman measurements. The $Z(YY)\bar{Z}$ and $X(YY)\bar{X}$ spectra are also identical.

The Raman bands of Gly-Gly crystal can be assigned on the basis of the Raman spectra of Gly-Gly in aqueous solution[5,21] and on the basis of the studies of *N*-methylacetamide[22] (NMA). Two very well resolved amide I bands (A-I) are located at *ca.* 1663 and 1622 cm^{-1} (see below for discussion of their splitting). Far from resonance with 488 nm excitation, the A-I doublet bands show equal intensities in the (*YY*) measurements. The band at 1622 cm^{-1} is slightly more intense than the band at 1663 cm^{-1} for the $Z(XY)\bar{Z}$ and $X(ZY)\bar{X}$ spectra; the inverse is true for the $Z(XX)\bar{Z}$ and $X(ZZ)\bar{X}$ spectra. Excitation close to resonance at 244 nm results in large changes in the spectral intensities. The A-I doublet band at 1663 cm^{-1} becomes more intense than the band at 1622 cm^{-1} and dominates the (*YY*) spectrum.

The amide II band (A-II) at *ca.* 1560 cm^{-1} is weak with visible excitation, but becomes strong with UV excitation. The Amide III (A-III) band at *ca.* 1261 cm^{-1} is strong with both visible and UV excitation. The strong band at *ca.* 1405 cm^{-1}, observed with both visible and UV excitation, sometimes resolved as a doublet, is the symmetric stretch of the carboxylate group.

The most intense band with visible excitation at *ca.* 962 cm^{-1} is assigned to carbon−carbon skeletal stretching. The relative intensity of this band dramatically decreases with UV excitation. Similar intensity differences occur between visible and UV excitation for the $C(4)H_2$ and $C(2)H_2$ methylene scissors deformation vibration[23] at *ca.* 1466 and 1435 cm^{-1}, respectively[24] (see Figure 1a for atom numbering scheme).

The Raman intensities in the laboratory coordinate system can be related to the diagonal molecular frame Raman tensor elements, r_1 and r_2, and the Euler's angles θ, φ, and χ, by eq A6 of Appendix A. We used the measured Raman intensities I_{XX}, $I_{XY} = I_{YX}$, I_{YY}, $I_{YZ} = I_{ZY}$, and I_{ZZ} for each vibrational band and eq A6 to solve numerically for the five unknowns r_1, r_2, θ, φ, and χ, using a least-squares fit criterion. A number of possible solution exist, as explained in Appendix A. We used the depolarization ratios measured for isotropic Gly-Gly aqueous solutions and eq A7 as an additional criterion, to find the unique set of r_1, r_2, θ, φ, and χ parameters. We rejected any solution which gave a depolarization ratio which differed by more than 3 standard deviations from the measured value for aqueous Gly-Gly.

The direction cosines between the three principal axes of the diagonal molecular Raman tensor, $\boldsymbol{\alpha}^{mol}$, and the laboratory coordinate system were calculated for each Raman band from the values of the Euler's angles θ, φ, and χ. Our laboratory coordinate system *XYZ* is related to the crystallographic Cartesian coordinate system, *abc*′ (where *c*′ is perpendicular to both the *a* and *b* crystallographic axes) by a 27° rotation about the $b = Y$ axis. We calculated the orientation of the principal axis

(20) (a) Porto, S. P. S. In *Light Scattering Spectra of Solids*; G. B. Wright, Ed.; Springer-Verlag: Berlin, 1969; Chapter A-1 (Light scattering with laser sources). (b) Damen, T. C.; Porto, S. P. S.; Tell, B. *Phys. Rev.* **1960**, *142*, 570. (c) Tell, B.; Damen, T. C.; Porto, S. P. S. *Phys. Rev.* **1966**, *144*, 771.

(21) Song, S.; Asher, S. A.; Krimm, S.; Shaw, K. D. *J. Am. Chem. Soc.* **1991**, *113*, 1155.

(22) (a) Chen X. G.; Asher S. A.; Schweitzer-Stenner, R.; Mirkin, N. G.; Krimm, S. *J. Am. Chem. Soc.* **1995**, *117*, 2884. (b) Chen X. G.; Schweitzer-Stenner, R.; Asher S. A.; Mirkin, N. G.; Krimm, S. *J. Phys. Chem.* **1995,** *99*, 3074.

(23) Tu, A. T. *Raman Spectroscopy in Biology;* John Wiley & Sons: New York, 1982; pp 27−71.

(24) These bands are assigned as scissor deformations, because their frequencies are close to the in-plane symmetric bending vibration of methylenes, which occur[23] at 1463 cm^{-1}.

Table 1. Molecular Raman Tensor Data of Amide and Carboxylate Vibrations in Gly-Gly Crystal

	visible				UV			
	A-I	A-II	A-III	COO^-	A-I	A-II	A-III	COO^-
$r_1 = \alpha_{xx}/\alpha_{zz}$	3.65	2.92	2.81	3.03	10.64	9.70	8.79	7.46
$r_2 = \alpha_{yy}/\alpha_{zz}$	−0.057	−0.49	−0.24	−1.62	0.41	−0.61	−0.077	−2.84
ρ^a	0.22	0.28	0.23	0.52	0.26	0.315	0.28	0.505
γ^b (deg)	31	55	57	56	41	60	60	69
δ^c (deg)	22	16	12	4	2	3	1	9

[a] Depolarization ratio. [b] Angle between *x* principal axis of Raman tensor and *b* crystallographic axis. [c] Angle between the plane of *x* and *z* principal axes of Raman tensor and amide plane.

Table 2. Correlation Diagram of Factor Group and Molecular Group

Isolated molecule	Site	Unit Cell
C_1	C_1	C_{2h}^6
(45A + 3r + 3t)	(45A +3r + 3t)	(90 + 12r) A_g(R)
		(90 + 12r) B_g(R)
		(90 + 11t +1a) A_u(IR)
		(90 + 10t +2a) B_u(IR)

of the Raman tensor (PART) in the *abc′* coordinate system by using a 27° rotation around the *b* axis and the values of the direction cosines of the principal axes of the molecular Raman tensor in the laboratory system.

The crystal structure shows that the *b* axis lies within the amide plane (within 3°) and is nearly parallel to the amide carbonyl bond (Figure 1). Thus, the amide plane lies almost perpendicular to the *ac* plane and forms a 58° angle to the *a* crystallographic axis (or 32° with the *X* laboratory axis). We used these angles to determine the angle δ between the amide plane and the plane containing the *x* and *z* principal Raman tensor axes. We used the software Siemens SHELXL (version 5.02) to determine the orientation of the PART relative to the Gly-Gly molecular geometry.

Table 1 shows the molecular Raman tensor data for the A-I (at 1663 cm^{-1}), A-II, A-III bands and for the carboxylate (COO^-) symmetric stretching band. Using a propagation of errors approach, we estimate a 3° maximum error for the PART orientation.

Discussion

Group Theoretical Discussion. The isolated Gly-Gly molecule point group is C_1. Gly-Gly has 45 internal vibrations, all of which are Raman (R) and infrared (IR) active. The crystal belongs to the space group $C_{2/c} = C_{2h}^6$. The 8 Gly-Gly molecules per unit cell must occupy a set of sites having a multiplicity of eight, which means that the site symmetry of the Gly-Gly molecules in the crystal is C_1, the same as that for the isolated molecule. Since the site symmetry group is a subgroup of the factor group C_{2h}^6, we can establish a correlation diagram between the isolated molecule group and the factor group[25] (Table 2).

According to the factor group analysis, the 8 molecules of Gly-Gly per unit cell will give rise to 360 internal vibrations, in addition to 24 rotation (r), 21 translation (t), and 3 acoustical modes (a). The factor group possesses an inversion center; thus, 180 *gerade* internal vibrations must be Raman active. Half belong to the irreducible representation A_g and the rest to B_g. Since the two-fold symmetry *b* crystallographic axis was chosen as the laboratory *Y* axis, 90 A_g internal vibrations should appear in the (*XX*), (*YY*), (*ZZ*), and (*XZ*) spectra,[25−27] while 90 B_g vibrations should appear in the (*XY*) and (*YZ*) spectra.

The visible and UV Raman spectra show far fewer bands; however, some of these bands show evidence of splitting. The A-I vibration is the most split, showing a doublet at *ca.* 1663 and 1622 cm^{-1} in all of the spectra.

The frequencies of the set of the A_g crystal Raman bands observed in the (*XX*), (*YY*), and (*ZZ*) Raman spectra are approximately the same as those of the B_g bands observed in the (*XY*) and (*YZ*) Raman spectra. This means that *correlation (Davydov) splitting* is insignificant, and we can utilize the *oriented gas model*[25] for our analysis of the hydrated Gly-Gly crystal.

The 12 molecules of H_2O per unit cell hydrogen-bond to the carboxylates and may serve to insulate the vibrations of the adjacent molecules. This probably minimizes the splitting of most of the Gly-Gly vibrations. In contrast, the amide hydrogen of each Gly-Gly molecule is directly hydrogen-bonded to the amide carbonyl of its neighbor. This results in a significant vibrational coupling for the A-I vibration, which has the largest contribution from C═O stretching.[22,23]

The eight Gly-Gly molecules in the unit cell have four unique orientations relative to the crystallographic axes. These different Gly-Gly orientations can be obtained by a C_2 rotation of a Gly-Gly molecule about the $b = Y$ crystallographic axis, by a reflection about the plane perpendicular to *b*, and by an inversion. We show below that each molecule contributes identically to the measured polarized crystal Raman spectra.

The Raman scattering tensors for vibrations of symmetry A_g and B_g can be written in the laboratory coordinate system[25−27] ($Y = b$):

$$\mathbf{A}_g = \begin{pmatrix} a & 0 & d \\ 0 & b & 0 \\ d & 0 & c \end{pmatrix} \qquad \mathbf{B}_g = \begin{pmatrix} 0 & e & 0 \\ e & 0 & f \\ 0 & f & 0 \end{pmatrix} \tag{1}$$

All the crystal symmetry operations leave the $\mathbf{A}_g$ tensor unchanged. The elements of the $\mathbf{B}_g$ tensor stay the same during inversion but change sign during the 180° rotation around the *b* axis or during the reflection in the plane perpendicular to the *b* axis. The Raman intensity scattered from each molecule is proportional to the square of the absolute value of the Raman tensor element (eq A3). Thus, the Raman intensities contributed by each molecule in the unit cell are identical.

The equivalent Raman scattering from each differently oriented molecule in the unit cell results in multiple solutions for the orientation of the PART within the molecular frame. For example, if the angle between the *b* crystallographic axis and the molecular axis PART of one molecule in the unit cell is 60°, then the three other molecules will have their corresponding PARTs at angles of −60°, 120°, and −120°. The orientation of the PART in the Gly-Gly molecule is fixed, and

(25) Turrell, G. *Infrared and Raman Spectra of Crystals;* Academic Press: London, 1972; pp 56−171.

(26) Loudon, R. *Adv. Phys.* **1964**, *13*, 423.

(27) Heine, V. *Group Theory in Quantum Mechanics;* Pergamon Press: New York, 1960; p 304.

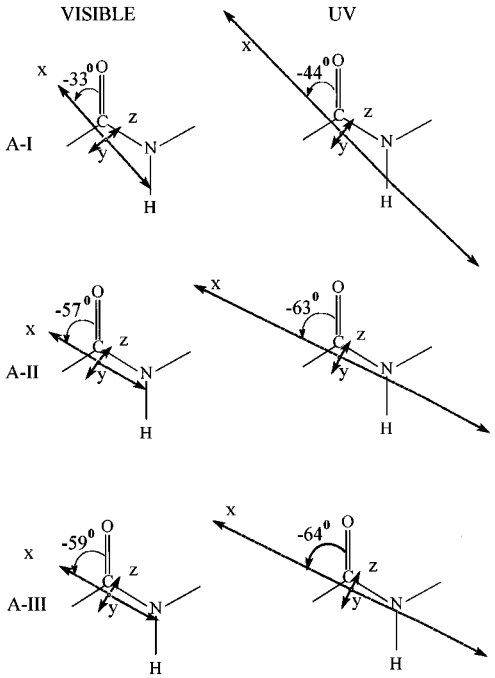

Figure 7. Representation of the orientation of the visible and UV excited principal axes of the Raman tensor (PART) for the amide vibrations. The angles are shown relative to the amide carbonyl bond. The lengths of the axes are proportional to magnitudes of the Raman tensor values. For visible excitation, the *y* axis is almost normal to the amide plane; for UV excitation, it is exactly normal to the amide plane.

we will have to use physical reasoning to choose the correct orientation of the PART within the molecule.

Orientation of Principal Raman Tensor Axes. Resonance Raman excitation within an isolated electronic transition causes the Raman scattering to be dominated by the transition moment of the resonant electronic transition. In this case, the major axis of the Raman tensor in the diagonal frame (MART) of each vibration will coincide with the electronic transition moment direction. The dominance by one transition can also occur in preresonance, and the orientation of the MART should be close to the electronic transition moment direction. This would clearly be the case for *N*-methylacetamide, whose A-II and A-III band Raman scattering, even with visible excitation, is dominated by its amide $\pi\rightarrow\pi^*$ transition.[22b]

The $\pi\rightarrow\pi^*$ amide (NV_1) transition[1] (also noted as $\pi_0\rightarrow\pi_-$ transition,[28] or $\pi_2\rightarrow\pi_3$ transition[29]) involves charge transfer of an electron from the N lone pair orbital to the antibonding π^* carbonyl orbital.[30] Therefore, the dipole transition moment should be directed from the N atom to the C═O bond. The MART of a vibration enhanced by the amide NV_1 electronic transition should lie parallel to this dipole transition moment and should occur along a line connecting the N atom to the carbonyl bond.

We will adopt Clark's transition moment convention[1] to describe the orientation of the MART in the molecular frame. The amide C═O bond is chosen as the reference axis in the peptide plane, and positive angles are defined by rotations towards the C—N bond (Figure 7). For the carboxylate group in the carboxylate plane, we use the C═O(1) bond as the reference axis, and the angle is positive if it is rotated toward the C—O(2) bond (Figure 8).

(28) Yan, J. F.; Momany, F. A.; Hofman, R.; Scheraga, H. A. *J. Phys. Chem.* **1970**, *74*, 420.
(29) Wang, Y.; Purrello, R.; Georgiou, S.; Spiro, T. G. *J. Am. Chem. Soc.* **1991**, *113*, 6368.
(30) Li, Y.; Garrell, R. L.; Houk, K. N. *J. Am. Chem. Soc.* **1991**, *113*, 5895.

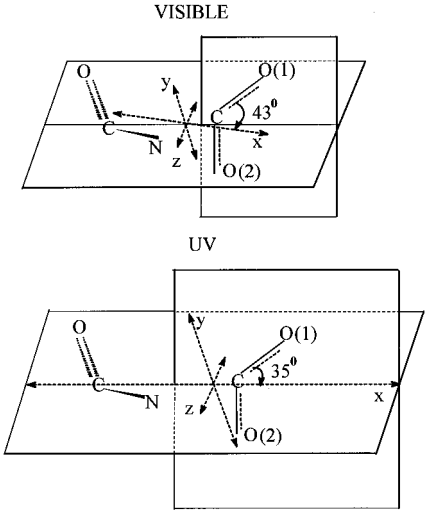

Figure 8. Orientation of the PART for the COO^- stretching vibration. The COO^- group lies in the figure plane.

The amide C═O bonds are oriented 4.5° from the *b* crystallographic axis (Figure 1a); thus, the four unique Gly-Gly crystal molecular orientations have the amide carbonyl bonds oriented at 4.5°, −4.5°, 175.5°, and −175.5° to the *b* axis. The orientation of the MART is identical for all molecules. Because the MART bisects the C(4)−C(3)−O(3) angle (see Figure 1a, and discussion below), the angle between MART and the C═O bond is *ca.* 4.5° greater than the angle γ between MART and the *b* axis (the exact difference depends on the value of δ given in Table 1).

Amide-I. With visible excitation, the 1663 cm^{-1} A-I vibration MART is inclined 33.3° from the C═O bond (Figure 7). Our calculated angle is similar to that Tsuboi *et al.*[8] reported for the 1667 cm^{-1} A-I band of aspartame with 488 nm excitation. We chose a negative angle, because with UV excitation, the angle increases to 44°, which we expect will lie approximately parallel to the amide $\pi\rightarrow\pi^*$ transition. This angle is almost identical to that of the amide $\pi\rightarrow\pi^*$ (NV_1) electronic transition relative to the C═O bond of myristamide[1,3] (−41°). Thus, we conclude that the A-I MART lies at −33° and −44° angles from the C═O bond with visible and 244 nm excitation, respectively (Figure 7). The 11° rotation of the MART from the visible to UV results from the fact that numerous electronic transitions are important in the A-I enhancement for visible excitation, and the MART is oriented between the dominating transitions. As resonance is approached, the MART enhancement becomes more dominated by the amide $\pi\rightarrow\pi^*$ NV_1 transition.

There are as many solutions for the MART orientation with respect to the crystallographic axes as there are uniquely oriented molecules in the unit cell. These solutions are connected by the symmetry operations, and the different Euler's angles for each solution have well-defined relationships. Physical reasoning is required in order to judge between them to determine the correct solution within the molecular frame; we utilized the MART angular change between the visible and UV excitation to determine the correct solution. Tsuboi *et al.*, indeed, chose the correct solution for the A-I band of aspartame[8] but did not indicate how they decided among the four possible solutions which occur for the aspartame $P4_1$ crystal, which has four molecules per unit cell.[31]

For visible excitation, the A-I MART (*x* axis) is oriented 6.5° from the amide plane (Table 3), and the angle between the plane

(31) Hatada, M.; Jancarik, J.; Graves, B.; Kim S. *J. Am. Chem. Soc.* **1985**, *107*, 4279.

Table 3. Orientation of Major Axis of the Raman Tensor (MART) of Amide and Carboxylate Vibrations in Gly-Gly Crystal[a]

	carbonyl C═O bond	amide plane	carboxylate plane	carboxylate C═O(1) bond
		Visible		
A-I	−33.3	6.5		
A-II	−56.9	11.9		
A-III	−59.3	9.7		
COO^-	−59.4	3.3	12.7	+43.1
		UV		
A-I	−44.1	0.5		
A-II	−63.2	1.0		
A-III	−63.7	1.4		
COO^-	−72.6	2.3	0.1	+35.0

[a] The data given are the angles (in degrees) between MART and the bond or plane identified in the column headings.

of the *x* and *z* principal Raman tensor axes and the amide plane is 22° (Table 1). With UV excitation, both the *x* and *z* axes rotate into the peptide plane (within experimental error).

The second 1622 cm^{-1} A-I band MART (not shown in the Table 3) is oriented at −31.0° to the C═O bond for visible excitation, which is an angle similar to that of A-I. The MART is only 4.7° out of the peptide plane. The *z* PART is almost in the peptide plane (only 1.5° off). For 244 nm excitation, the MART lies at an angle of −45.7° with the C═O bond and lies in the amide plane, the same orientation as for the 1663 cm^{-1} A-I band. However, for UV excitation, the *z* PART lies 39° out of the amide plane.

Amide-II and Amide-III Bands. The A-II and A-III bands at *ca.* 1560 and 1261 cm^{-1}, respectively, contain significant C−N stretching and N−H bending. The A-II band is very weak with visible excitation, in contrast to the A-III band, but its intensity is still sufficient to determine its Raman tensor elements. Both the A-II and A-III bands are strongly enhanced with 244 nm excitation. The orientations of their PARTs are essentially identical.

We determined angles of −56.3° and −59.3° between the A-II and A-III MARTs and the C═O bond with visible excitation (Figure 7). The A-III MART angle differs in orientation from that measured by Tsuboi *et al.*,[8] who reported an angle of +56° between the C═O bond and the A-III MART of aspartame (excited at 488 nm). We believe that, for this case, Tsuboi *et al.* chose the incorrect solution.

Tsuboi presupposed that the A-III MART would bisect the C═O and C−N bonds, because he expected the A-III MART to be nearly perpendicular to that of the A-I vibration.[32] Both orientations of the A-III MART (positive or negative angle) relative to the *b* crystallographic axis are possible solutions.

We were able to choose the correct solution because we know that the amide II and III bands are dominantly preresonance enhanced by the amide $\pi\rightarrow\pi^*$ transition, even for visible excitation.[33] Thus, the MART of the amide II and III bands must lie approximately parallel to the direction of the amide $\pi\rightarrow\pi^*$ transition, which lies approximately along a line from the nitrogen to the carbonyl bond.

Little change occurs in the MART orientation relative to the C═O bond upon UV excitation; the MART angle to the C═O bond is the same for both bands, −63.2° for A-II and −63.7° for A-III (Figure 7).

Our calculations show that, with visible excitation, the A-III MART (9.7°) and the *z* PART (7.9°) axes lie out of the peptide plane. For the A-II band, the angles are similar, at 11.9° and 10.1°, respectively. With UV excitation, the MART and *z* PART lie within the peptide plane within experimental error.

COO^- Stretching Vibration. The carboxylate symmetric stretching band at 1405 cm^{-1} is strong with both visible and UV excitation. We calculate a diagonal Raman tensor with three elements, the second largest one of which is negative (Table 1). Use of this tensor to calculate the isotropic depolarization ratio results in values of 0.52 and 0.505 with 488 and 244 nm excitation, respectively, which are very close to those measured for aqueous solution samples.[5] This indicates that at least three transitions are significant in the enhancement of the carboxylate symmetric stretching vibration, which gives rise to the observed diagonal Raman polarizability tensor ellipsoid ratio of 7.46:−2.84:1.00 (Table 1).

The plane containing the COO^- group is oriented 40.7° to the peptide plane. The COO^- stretching vibration MART lies almost along the line of intersection of the peptide and carboxylate planes. With visible excitation, the COO^- stretching vibration MART lies only 3.3° out of the peptide plane and 12.7° out of the COO^- plane. With UV excitation, the MART lies exactly in the COO^- plane, and only 2.3° out of the amide plane. The observed UV orientation of the MART, in a line connecting the carboxylate and amide groups, is consistent with the proposed dominant enhancement of the carboxylate stretch by a charge transfer transition from a nonbonding COO^- orbital to the amide π^* orbital.[5]

The COO^- stretching MART occurs at an angle of −59.4° to the C═O bond of the amide with visible excitation; this angle increases to −72.6° with UV excitation (Table 3). The COO^- stretching MART makes a 43.1° angle with the carboxylate C═O(1) bond with visible excitation, which decreases to 35.0° with UV excitation (Figure 8).

The COO^- stretching vibration is unique in having its α_{yy} element larger in absolute value than the α_{zz} element, which is normalized to 1.0. With UV excitation, the MART lies in the intersection of the amide and carboxylate planes and is tilted by 35.0° from the amide C═O bond. The *y* and *z* axes are nearly bisected by the COO^- plane; the *y* and *z* axes form angles of 40.4° and 49.6° with the COO^- plane, respectively, with UV excitation. The relative signs and orientation of the carboxylate Raman tensor elements can be qualitatively rationalized by the results of Chen *et al.*[5] The carboxylate stretch is most strongly enhanced by the charge transfer transition, which results in the MART oriented along the intersection between the carboxylate and amide planes. The carboxylate $\pi\rightarrow\pi^*$ transition contributes a Raman tensor element of sign opposite to that of the charge transfer transition.[5] These two transitions alone result in a Raman ellipse oriented in the carboxylate plane. A third transition, probably the amide $\pi\rightarrow\pi^*$ transition, contributes enhancement with a Raman tensor element of sign opposite to that of the carboxylate $\pi\rightarrow\pi^*$ transition and with a transition moment within the amide plane. This results in three significant tensor elements, in which the smaller *y* and *z* axes are oriented out of the amide and carboxylate planes.

Relation of the Orientation of the PART to the Electronic Transition Moments. The Raman tensor elements are related to the electronic transition moments in the KDH theory, as[34]

$$(\alpha_{\epsilon\eta})_{I\rightarrow F} = \sum_V \frac{\langle F|m_\epsilon|V\rangle\langle V|m_\eta|I\rangle}{E_V - E_I - E_L - i\Gamma} + \frac{\langle F|m_\epsilon|V\rangle\langle V|m_\eta|I\rangle}{E_V - E_F + E_L - i\Gamma} \quad (2)$$

where $|I\rangle$, $|V\rangle$, and $|F\rangle$ are the initial, intermediate, and final vibronic states with energies E_I, E_V, and E_F. Γ is the

(32) Tsuboi, M. *J. Polym. Sci.* **1962**, *59*, 139.

(33) Dudik, J. M.; Johnson, C, R.; Asher, S. A. *J. Phys. Chem.* **1985,** *107,* 3805.

(34) Myers, A. B.; Mathies, R. A. In *Biological Applications of Raman Spectroscopy*; Spiro, T. G., Ed.; Resonance Raman Intensities: A Probe of Excited-State Structure and Dynamics; John Wiley & Sons Inc.: New York, 1987; Vol. 2, Chapter 1, pp 1−58.

homogeneous line width, and m_ϵ is a vector component of the transition dipole moment operator. $\epsilon,\eta = x,y,z$ in the molecular Cartesian coordinate system.

Resonance with only one nondegenerate electronic transition causes all but one of the transition moment matrix elements to vanish. We chose the remaining transition moment to lie along the *x*-axis (only $\alpha_{xx} \neq 0$). As a result, the *x* MART points along the transition moment of the resonant electronic transition. (The case of two electronic transitions is treated below.)

One electronic transition can also dominate the preresonance Raman spectra. For example, the *N*-methylacetamide *ca*. 190 nm $\pi\rightarrow\pi^*$ transition dominates the Raman intensity, even with excitation in the visible spectral region. In fact, the isotropic solution depolarization ratio is nearly 0.33 with excitation from the near IR into the UV;[22b] one element of the diagonal frame Raman tensor dominates, and the direction of the *x* axis (MART) is parallel to the direction of the *ca*. 190 nm $\pi\rightarrow\pi^*$ electronic transition moment.

Estimation of Amide $\pi\rightarrow\pi^*$ Transition Moment Orientation. We can obtain a very rough estimate of the amide $\pi\rightarrow\pi^*$ transition moment orientation by neglecting the α_{yy} and α_{zz} elements and by assuming that the transition moment lies along the MART. For the A-III band, we calculate an angle of $-63.7°$ between the amide $\pi\rightarrow\pi^*$ transition moment and the amide C═O bond, which is not far from the value of $-55° \pm 5°$ given by Clark for the amide $\pi\rightarrow\pi^*$ transition in *N*-acetylglycine.[1] We get a similar result from the A-II vibration. The A-I band gives a value of $-44.1°$, which is identical to that in myristamide[1,3] ($-41°$) and in propanamide[1] ($-35° \pm 3°$).

The different values of the amide $\pi\rightarrow\pi^*$ transition moment orientations calculated from the A-I or A-III bands result from the fact that more than one electronic transition is involved in the enhancement of the amide vibrations.

This is only a rough estimate since the measured *preresonance* Raman tensors have non-negligible values for the other two tensor elements; as a result, the orientation of the MART lies at an angle to the dominant electronic transition moment direction, which depends on the magnitude of enhancement of the other transitions and the angle between the transitions (see eqs 4−6, below).

Determination of Orientations of Amide $\pi\rightarrow\pi^*$ and Charge Transfer Transition Moments. We can determine the molecular orientations of the amide $\pi\rightarrow\pi^*$ and charge transfer (CT) transition moments by utilizing the two measured dominant tensor element values and by decomposing the Raman tensor into separate contributions from the transitions. We can define two coordinate system $x_1y_1z_1$ and $x_2y_1z_2$, with x_1 parallel to electronic transition moment M_1 and x_2 parallel to electronic transition moment M_2. The Raman tensor associated with the individual electronic transition moments are written in their respective frames as

$$\boldsymbol{\alpha}_1 = \begin{pmatrix} \alpha_1 & 0 & 0 \\ 0 & 0 & 0 \\ 0 & 0 & 0 \end{pmatrix} \qquad \boldsymbol{\alpha}_2 = \begin{pmatrix} \alpha_2 & 0 & 0 \\ 0 & 0 & 0 \\ 0 & 0 & 0 \end{pmatrix} \tag{3}$$

We can express the total Raman tensor $\boldsymbol{\alpha}$ in the first frame by rotating the second frame by the angle β (between M_1 and M_2), around the y_1 axis perpendicular to the plane defined by M_1 and M_2, and adding it to the first one. $\boldsymbol{\alpha}$ is not diagonal and is diagonalized by a rotation with an angle ζ around y_1 to give a tensor with only two diagonal elements (see Figure 9). The details of this calculation can be found in the work of Chen *et al*.[5] The Raman tensor element relationships are

$$\alpha_{xx} + \alpha_{zz} = \alpha_1 + \alpha_2 \tag{4}$$

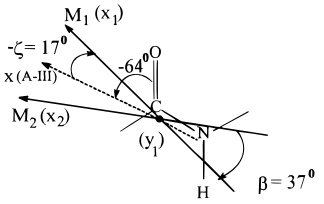

Figure 9. Orientation of the amide $\pi\rightarrow\pi^*$ (M_1) and charge transfer (M_2) transition moments.

$$\alpha_{xx}\alpha_{zz} = \alpha_1\alpha_2 \sin^2\beta \tag{5}$$

$$\zeta = {}^1/_2 \tan^{-1}\{-\alpha_2 \sin(2\beta)/[\alpha_1 + \alpha_2 \cos(2\beta)]\} \tag{6}$$

ζ is the angle that the MART is rotated from the direction of M_1. Thus, from ζ we can calculate the orientation of the dominant electronic transition moment, M_1. The angle β allows us to calculate the orientation of the second electronic transition moment, M_2. The results of this calculation for the A-III band should be accurate, since $\alpha_{yy} \approx 0$ ($\alpha_{yy} = -0.077$).

We determined the relative values of α_1 and α_2 from measurements of the Raman cross sections of the A-III bands of *N*-methylacetamide (NMA) and Gly-Gly. The A-III bands are at similar frequencies, and the normal modes are expected to be very similar.[5,22] We recently demonstrated through the absorption difference spectrum that the absorption spectrum of Gly-Gly can be modeled as the sum of NMA-like amide $\pi\rightarrow\pi^*$ and charge transfer transitions.[5] The absorption frequency, the molar absorptivity, and the band shape of the Gly-Gly amide $\pi\rightarrow\pi^*$ transition are close to those of NMA. Thus, we can obtain α_1 from our measurements of the Raman cross section of NMA at 244 nm.

The Raman cross section, σ, can be related to the two Raman tensor invariants,[35] a' and $(\gamma')^2$ as

$$\sigma \propto [45(a')^2 + 7(\gamma')^2] \tag{7}$$

where $a' = {}^1/_3(\alpha_{xx} + \alpha_{yy} + \alpha_{zz})$ and $(\gamma')^2 = {}^1/_2[(\alpha_{xx} - \alpha_{yy})^2 + (\alpha_{yy} - \alpha_{zz})^2 + (\alpha_{zz} - \alpha_{xx})^2]$ using the diagnolized Raman tensor elements.

For NMA, only $\alpha_1 \neq 0$. Thus, the ratio of the Raman cross section of Gly-Gly and NMA can be written

$$\frac{\sigma_{\text{Gly-Gly}}}{\sigma_{\text{NMA}}} = \frac{45(\alpha'_{\text{Gly-Gly}})^2 + 7(\gamma'_{\text{Gly-Gly}})^2}{12\alpha_1^2} = 2.9 \tag{8}$$

where the ratio value 2.9 is obtained from the Raman cross sections with 244 nm excitation.[5] Since we know the values of $(a')^2$ and $(\gamma')^2$ from the A-III molecular Raman tensor, we use eq 8 to obtain $\alpha_1 = 5.23$ for the amide $\pi\rightarrow\pi^*$ transition. Substitution into eqs 4−6 gives $\alpha_2 = 4.56$, $\beta = 37.4°$, and $\zeta = -17.2°$.

Thus, the A-III band MART is rotated by $-17.2°$ from the direction of M_1 (Figure 9). Hence, the amide $\pi\rightarrow\pi^*$ (NV_1) transition moment, M_1, is oriented at $-46.5° \pm 3°$ from the amide C═O bond. Within experimental error, this angle is identical to that obtained by polarization absorption measurements of the amide NV_1 transition in myristamide[3] but is a little higher than the $-35°$ reported for propanamide.[1] We calculate that the charge transfer transition moment in Gly-Gly is tilted $-83.9° \pm 3°$ from the C═O bond (Figure 9).

If we utilize the same approach for the A-II band, where the Raman cross section ratio for Gly-Gly and NMA is 3.6 with 244 nm excitation,[5] we obtain $\beta = 35.6°$ and $\zeta = -18.0°$,

(35) Long, D. A. *Raman Spectroscopy;* McGraw-Hill: New York, 1977; p 83.

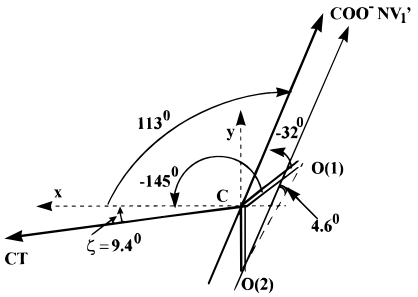

Figure 10. Orientation of the carboxylate $\pi\rightarrow\pi^*$ (NV_1') transition moment.

which results in angles of $-45.2° \pm 3°$ for the amide $\pi\rightarrow\pi^*$ (NV_1) transition and $-80.8° \pm 3°$ for the charge transfer transition from the C═O bond. These angles are almost identical to those calculated from the A-III band. In this calculation, we have safely assumed that the electronic transition moments giving rise to enhancement are in the amide plane and contribute to α_{xx} and α_{zz} but not to α_{yy}, which is perpendicular to the amide plane. The electronic transition moments out of the amide plane mostly contribute to α_{yy}; their contributions to α_{xx} and α_{zz} are considered negligible.

The orientation of the A-I MART is $-44°$ from the amide C═O bond, and is almost parallel to our calculated amide $\pi\rightarrow\pi^*$ (NV_1) transition moment at $-46°$. This suggests that the A-I band is dominantly resonance enhanced by the amide $\pi\rightarrow\pi^*$ (NV_1) electronic transition moment at *ca*. 185 nm, even with preresonance excitation at 244 nm. It is satisfying that the second largest PART (*z*) is oriented at $+46°$ to the carbonyl bond, which is the orientation ($+46 \pm 8°$) proposed by Clark's measurements for the second amide $\pi\rightarrow\pi^*$ (NV_2) transition.

For 244 nm excitation, the COO^- stretching MART is orientated $-72.6°$ to the amide C═O bond, which is only 9.4° from the charge transfer moment direction. The carboxylate vibration has significant values for all three diagonal tensor elements. We can attempt to very approximately estimate the angle of the next most important transition by utilizing the value $+9.4°$ for the value of ζ in eqs 4−6 to estimate the carboxylate $\pi\rightarrow\pi^*$ (NV_1') transition moment orientation. If we consider the charge transfer transition as M_1 and the carboxylate NV_1' transition as M_2, the angle β should be negative. The calculations are done in the *xy* plane, which is at an angle of 40.7° to the COO^- plane. Two solutions occur: $\alpha_1 = -2.95$, $\alpha_2 = 7.57$, and $\beta = -102.9°$, or $\alpha_1 = 8.24$, $\alpha_2 = -3.62$, and $\beta = -122.9°$.

The reasonable choice is the one where α_1 is the largest value. The value of $\beta = -122.6°$ indicates that the angle between the carboxylate NV_1' and the MART of the COO^- stretching vibration is $-\beta - \zeta = -(-122.6°) - 9.4° = 113.2°$ (Figure 10). This result predicts that, as excitation occurs farther into the UV, the angle between the *xy* and carboxylate planes will decrease, until the *xy* plane becomes parallel to the carboxylate plane for resonance with the carboxylate $\pi\rightarrow\pi^*$ (NV_1') transition.

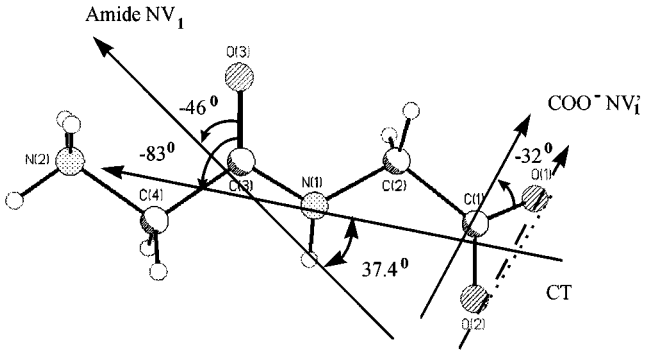

Figure 11. Orientation of the electronic transition moments of glycylglycine.

The angle between the COO^- stretch MART and the C═O-(1) bond is $+35°$, or $-145°$ (see Figure 10). Thus, the carboxylate NV_1' transition moment will lie in the carboxylate plane at an angle $-32°$ to the C═O(1) bond. This orientation is parallel (only 4.6° off) to the line connecting the carboxylate oxygens, which is the orientation of the $\pi\rightarrow\pi^*$ transition moment of formate ion.[3] This gives strong support to the utility of the approximations we have used. Figure 11 summarizes the orientations we calculate for the electronic transition of glycylglycine.

Conclusion

We have demonstrated the utility of near-resonance single-crystal Raman measurements to determine the orientation of the transition moments of the resonant excited state and the next closest excited state. For gylcylglycine we have determined that the transition moment of the amide $\pi\rightarrow\pi^*$ transition (NV_1) lies in the amide plane at an angle of $-46° \pm 3°$ from the amide carbonyl bond. The charge transfer transition at *ca*. 200 nm has its transition moment oriented almost along the line of intersection of the amide and carboxylate planes at $-83° \pm 3°$ from the amide carbonyl bond. The carboxylate $\pi\rightarrow\pi^*$ transition (NV_1') is oriented almost parallel to a line connecting the carboxylate oxygen atoms. These transition moment orientations occur for a glycylglycine crystal where the carboxylates are hydrated and the amide groups are hydrogen-bonded in a β-sheet-like structure. This amide $\pi\rightarrow\pi^*$ transition orientation is likely to be that commonly occurring for amides in peptides and proteins, while the orientation of the charge transfer transition and the carboxylate $\pi\rightarrow\pi^*$ transition is likely to be that found within the penultimate carboxylate end of peptides and proteins.

Acknowledgment. We gratefully acknowledge support from NIH Grant R01GM30741-13 to S.A.A. We also thank Prof. Brian M. Craven from the Department of Crystallography for kind help in indexing the crystal faces.

Appendix A

Let us suppose that *XYZ* is the laboratory axis system, and *xyz* is the molecule-fixed axis system. If the Raman tensor of a constituent molecule in the frame *xyz* is $\boldsymbol{\alpha}^{mol}$, the Raman tensor in the laboratory system $\boldsymbol{\alpha}^{lab}$ is obtained by

$$\boldsymbol{\alpha}^{lab} = \mathbf{R}^T\boldsymbol{\alpha}^{mol}\mathbf{R} \tag{A1}$$

where $\mathbf{R}$ is the orthogonal rotation matrix

$$\mathbf{R} = \begin{bmatrix} \cos\theta\cos\varphi\cos\chi - \sin\varphi\sin\chi & -\cos\theta\cos\varphi\sin\chi - \sin\varphi\cos\chi & \sin\theta\cos\varphi \\ \cos\theta\sin\varphi\cos\chi + \cos\varphi\sin\chi & -\cos\theta\sin\varphi\sin\chi + \cos\varphi\cos\chi & \sin\theta\sin\varphi \\ -\sin\theta\cos\chi & \sin\theta\sin\chi & \cos\theta \end{bmatrix} \tag{A2}$$

and θ, φ, and χ are the Euler's angles.[36] $\mathbf{R}^T$ is the transpose matrix of **R**. The elements of the **R** matrix are direction cosines relating the nonrotated system to the rotated system. We are transforming the Raman tensor from the constituent molecule (rotating axes) to the laboratory system (nonrotating axes), so our **R** matrix is the transpose of the matrix defined by Wilson, Decius, and Cross.[36]

The Raman intensity from the scattering molecules within the probe volume element is[25]

$$I_{es} = A|e_e{}^T \boldsymbol{\alpha}^{lab} e_s|^2 \qquad e, s = X, Y, Z \tag{A3}$$

where e_e and e_s are the unit vectors which define the direction of the electric field of the exciting and scattered radiation, respectively. A is a constant.[37] As discussed above (see Group Theoretical Discussion), different molecules in the unit cell usually have different values for $\boldsymbol{\alpha}^{lab}$, but the quantity $|e_e{}^T\boldsymbol{\alpha}^{lab}e_s|^2$ is identical for all molecules in the crystal. From eqs A1 and A3, the Raman intensity can be written

$$I_{es} = A|e_e{}^T \mathbf{R}^T \boldsymbol{\alpha}^{mol} \mathbf{R}\, e_s|^2 \qquad e, s = X, Y, Z \tag{A4}$$

When the molecular Raman tensor $\boldsymbol{\alpha}^{mol}$ is symmetric, it can be written in the diagonal frame by a suitable choice of the *xyz* coordinate system attached to the molecule. The diagonal tensor, $\boldsymbol{\alpha}^{mol}$, can be written

$$\boldsymbol{\alpha}^{mol} = \begin{pmatrix} \alpha_{xx} & 0 & 0 \\ 0 & \alpha_{yy} & 0 \\ 0 & 0 & \alpha_{zz} \end{pmatrix} = \alpha_{zz} \begin{pmatrix} r_1 & 0 & 0 \\ 0 & r_2 & 0 \\ 0 & 0 & 1 \end{pmatrix} \tag{A5}$$

where $r_1 = \alpha_{xx}/\alpha_{zz}$ and $r_2 = \alpha_{yy}/\alpha_{zz}$.

The *x*, *y*, and *z* axes are the principal axis of the molecular Raman scattering tensor (PART). If we write $A(\alpha_{zz})^2 = K$, then eq A4 becomes

$$I_{es} = K|e_e{}^T \mathbf{R}^T \boldsymbol{\alpha}^{mol} \mathbf{R}\, e_s|^2 \qquad e, s = X, Y, Z \tag{A6}$$

which relates the measured Raman intensities in the laboratory coordinate system to the diagonal Raman tensor elements r_1 and r_2. Equation A6 involves six second-order transcendental equations which do not possess a unique solution for the unknowns r_1, r_2, θ, φ, χ, and K. By normalizing the Raman intensities, K disappears in the explicit equations, and we can use five oriented polarized Raman intensities measured in the laboratory coordinate system to solve numerically five equations for the five unknowns r_1, r_2, θ, φ, and χ, using a least-squares fit criterion.

We choose the correct solution by requiring that r_1 and r_2 give the experimentally observed value ρ of the isotropic solution depolarization ratio:[8]

$$\rho = \frac{1.5[(r_1 - r_2)^2 + (r_2 - 1)^2 + (1 - r_1)^2]}{5(r_1 + r_2 + 1)^2 + 2[(r_1 - r_2)^2 + (r_2 - 1)^2 + (1 - r_1)^2]} \tag{A7}$$

The PART orientation is calculated from the direction cosines in the laboratory coordinate system; each row of the orthogonal matrix **R** (see eq A2) gives the direction cosines of the *x*, *y*, and *z* PART in the laboratory system.

Appendix B

Here we consider the more general case, where the optic plane is perpendicular to the *b* crystallographic axis of the monoclinic crystal, but where the OP_1 and OP_2 optic axes are not mutually perpendicular.

The laboratory *Y* axis is oriented along the *b* crystallographic axis. The laboratory *Z* axis is oriented parallel to the OP_1 optic axis by rotating the Cartesian crystallographic system *abc*′ by an angle ϖ about the $b = Y$ axis:

$$\mathbf{R}_Y(\varpi) = \begin{pmatrix} \cos\varpi & 0 & \sin\varpi \\ 0 & 1 & 0 \\ -\sin\varpi & 0 & \cos\varpi \end{pmatrix} \tag{B1}$$

thus,

$$\boldsymbol{\alpha}^{lab}(\varpi) = \mathbf{R}_Y{}^T(\varpi)\alpha^{cry}\mathbf{R}_Y(\varpi) \tag{B2}$$

where $\boldsymbol{\alpha}^{cry} = \mathbf{A}_g'$ or $\mathbf{B}_g'$, which are the Raman tensors for the A_g and B_g molecular vibrations in the *abc*′ Cartesian crystallographic system. $\mathbf{A}_g'$ and $\mathbf{B}_g'$ can be written[25,26]

$$\mathbf{A}_g' = \begin{pmatrix} a' & 0 & d' \\ 0 & b' & 0 \\ d' & 0 & c' \end{pmatrix} \tag{B3}$$

$$\mathbf{B}_g' = \begin{pmatrix} 0 & e' & 0 \\ e' & 0 & f' \\ 0 & f' & 0 \end{pmatrix} \tag{B4}$$

For an A_g vibration, the Raman tensor elements in the laboratory system are

$$\alpha_{XX} = a' \cos^2\varpi + c' \sin^2\varpi - d' \sin(2\varpi) \tag{B5a}$$

$$\alpha_{XY} = \alpha_{YX} = 0 \tag{B5b}$$

$$\alpha_{YY} = b' \tag{B5c}$$

$$\alpha_{YZ} = \alpha_{ZY} = 0 \tag{B5d}$$

$$\alpha_{XZ} = \alpha_{ZX} = (a' - c') \sin\varpi \cos\varpi + d' \cos(2\varpi) \tag{B5e}$$

$$\alpha_{ZZ} = a' \sin^2\varpi + c' \cos^2\varpi + d' \cos(2\varpi) \tag{B5f}$$

and those for a B_g vibration should be

$$\alpha_{XY} = \alpha_{YX} = e' \cos\varpi - f' \sin\varpi \tag{B6a}$$

$$\alpha_{YZ} = \alpha_{ZY} = e' \sin\varpi + f' \cos\varpi \tag{B6b}$$

with other elements equal to zero.

We can measure the $I_{XX}(\varpi)$, $I_{YY}(\varpi) = (b')^2$, and $I_{XY}(\varpi)$ Raman spectra with the excitation propagating parallel to the optic axis OP_1. Measurements with the excitation propagating parallel along the other optic axis, OP_2, occur upon rotating the crystal around the $b = Y$ axis by an angle ϖ'. Thus, we measure $I_{XX}(\varpi')$, $I_{YY}(\varpi') = I_{YY}(\varpi) = (b')^2$, and $I_{XY}(\varpi')$.

Thus, we obtain five values for the intensities. If we want to determine all six Raman tensor elements for the A_g and B_g vibrations a', b', c', d', e', and f', we must carry out another measurement with the exciting light parallel to the optic axis $OP_1 = Z$. We rotate the crystal around *Z* with an angle ξ. Since *Z* is an optic axis, the polarization of the exciting and scattered light unaffected by this rotation. The rotation matrix can be written

$$\mathbf{R}_Z(\xi) = \begin{pmatrix} \cos\xi & \sin\xi & 0 \\ -\sin\xi & \cos\xi & 0 \\ 0 & 0 & 1 \end{pmatrix} \tag{B7}$$

The laboratory Cartesian system is related to the crystallographic Cartesian system by two consecutive rotations: the

(36) Wilson, E. B., Jr.; Decius, J. C.; Cross, P. C. *Molecular Vibration;* Dover: New York, 1980; pp 285−286.
(37) Asher, S. A. *Annu. Rev. Phys. Chem.* **1988**, *39*, 537.

first rotation around axis *Y*, $\mathbf{R}_Y(\varpi)$, and the second one around axis *Z*, $\mathbf{R}_Z(\xi)$. The whole rotation $\mathbf{R}(\xi,\varpi) = \mathbf{R}_Z(\xi)\mathbf{R}_Y(\varpi)$ is isomorphic with the product of matrices B7 and B1:

$$\mathbf{R}(\xi,\varpi) = \begin{pmatrix} \cos\xi\cos\varpi & \sin\xi & \cos\xi\sin\varpi \\ -\sin\xi\cos\varpi & \cos\xi & -\sin\xi\sin\varpi \\ -\sin\varpi & 0 & \cos\varpi \end{pmatrix} \quad \text{(B8)}$$

The tensor in the laboratory system is related to the tensor in the crystallographic system by

$$\boldsymbol{\alpha}^{\text{lab}}(\xi,\varpi) = \mathbf{R}^{\text{T}}(\xi,\varpi)\boldsymbol{\alpha}^{\text{cry}}\mathbf{R}(\xi,\varpi) \quad \text{(B9)}$$

From eq B9, we find that the tensor element, e.g., $\alpha(\xi,\varpi)_{YY}$, obtained from an A_g vibration can be written

$$\alpha(\xi,\varpi)_{YY}{}^{A} = a' \sin^2\xi + b' \cos^2\xi \quad \text{(B10)}$$

and that from a B_g vibration should be

$$\alpha(\xi,\varpi)_{YY}{}^{B} = e' \sin(2\xi) \quad \text{(B11)}$$

Similar equations can be written for other tensor elements.

We find that the vibrations of the Gly-Gly crystal are essentially degenerate. Thus, the measured Raman intensity is the sum of that of the A_g and B_g vibrations. Thus, the measured intensity can be written

$$I_{YY}(\xi,\varpi) = [\alpha(\xi,\varpi)_{YY}{}^{A}]^2 + [\alpha(\xi,\varpi)_{YY}{}^{B}]^2 \quad \text{(B12)}$$

Equations B5a−f, B6a,b, written for two different angles of rotation, ϖ and ϖ', together with eq B12, after the substitution of the eqs B10 and B11, yield the values of all the tensors elements a', b', c', d', e', and f', by solving the following equations:

$$I_{XX}(\varpi) = [a' \cos^2\varpi + c' \sin^2\varpi + d' \sin(2\varpi)]^2 \quad \text{(B13a)}$$

$$I_{XX}(\varpi') = [a' \cos^2\varpi' + c' \sin^2\varpi' + d' \sin(2\varpi')]^2 \quad \text{(B13b)}$$

$$I_{YY}(\varpi) = (b')^2 \quad \text{(B13c)}$$

$$I_{XY}(\varpi) = [e' \cos\varpi - f' \sin\varpi]^2 \quad \text{(B13d)}$$

$$I_{XY}(\varpi') = [e' \cos\varpi' - f' \sin\varpi']^2 \quad \text{(B13e)}$$

$$I_{YY}(\xi,\varpi) = [a' \sin^2\xi + b' \cos^2\xi]^2 + [e' \sin(2\xi)]^2 \quad \text{(B13f)}$$

By analytically solving these five eqs B.13a−f, we determine the five unknowns a′, b', c', d', e', and f'. As those equations are of the second order, the solution is not unique. The square of the above tensors elements give us the intensities $I_{aa} = (a')^2$, $I_{ab} = (e')^2$, $I_{bb} = (b')^2$, $I_{bc'} = (f')^2$, $I_{c'c'} = (c')^2$, and $I_{c'a} = (d')^2$. We can use these intensities to solve numerically eqs A6, with $e, s = a, b, c'$. The same procedure, described in Appendix A and in the paper, can be used to calculate the Raman tensor elements in a diagonal frame and the orientation of the PART of the molecule in question.

JA961725Z